

Uncertainties of Sudakov form factors

Stefan Gieseke

*Institut für Theoretische Physik
Universität Karlsruhe, 76128 Karlsruhe, Germany
gieseke@particle.uni-karlsruhe.de*

ABSTRACT: We study the uncertainties of Sudakov form factors as the basis for parton shower evolution in Monte Carlo event generators. We discuss the particular cases of systematic uncertainties of parton distribution functions and scale uncertainties.

KEYWORDS: Quantum Chromodynamics, Monte Carlo Event Generator, Parton Shower, Parton Distribution Functions.

Contents

1. Introduction	1
2. Sudakov form factor for space-like branchings	2
3. Numerical study	5
4. Results	6
4.1 Different initial conditions	6
4.2 MRST vs CTEQ	7
4.3 Parametrization of α_S	7
4.4 Larger cutoff	8
5. Conclusion	8

1. Introduction

The simulation of final states in the collision of highly energetic particles at current and future colliders is largely based upon parton shower evolution models. The theoretical foundation of these models is the interpretation of Sudakov form factors as no-emission probabilities [1, 2]. For hadronic collisions, the space-like evolution of initial state partons from the hard scale Q_h of the partonic subprocess and relatively small x is 'guided' by the ratio of parton distribution functions (pdf's) [3]. In this paper we would like to address the effect of uncertainties in the Sudakov form factors as a result of pdf uncertainties [4, 5]. We shall compare this effect to the uncertainty due to the choice of scale in the strong coupling constant α_S . We choose to use the Sudakov form factors that are going to be used for the initial state evolution in future versions of **Herwig++** [6]. The conclusion should qualitatively remain the same for the Sudakov form factors that results from different kinematical variables in the programs **HERWIG** [7] and **PYTHIA**[8] or the new program **SHERPA** [9]. They may, however, differ in details as the different kinematics will lead to emphasis on different regions of evolution phase space.

Furthermore we limit our discussion to the case of spacelike evolution. The estimated size of uncertainties due to effects like scale variation in $\alpha_S(Q)$ should be similar in the case of timelike evolution. As the pdf's only appear in spacelike evolution we can study all effects of our interest here. Another limitation is the

discussion of the uncertainties due to terms in the Sudakov form factor that are formally subleading in the sense of the next-to-leading (soft and/or collinear) logarithmic approximation. Formally we may add or subtract terms in the splitting functions that give rise to only non-logarithmic terms after integration over \tilde{q} (see below). Adjusting these terms can be crucial for matching of matrix elements and parton showers in the CKKW scheme [10, 11] as discussed in [12, 13]. The effect, however, appears to be mostly of technical importance close to the matching scale inherent to this kind of matching scheme.

2. Sudakov form factor for space-like branchings

The Sudakov form factor for spacelike backward evolution of a parton a from the hard scale \tilde{q}_{\max} down to some scale \tilde{q} can be written as [2, 3]

$$S_a(\tilde{q}, \tilde{q}_{\max}; x, \tilde{q}_0) = \exp \left[- \sum_b \mathcal{I}_{ba}(\tilde{q}, \tilde{q}_{\max}; x, \tilde{q}_0) \right]. \quad (2.1)$$

The sum on the right hand side (rhs) is over all possible splittings into partons of type b and

$$\mathcal{I}_{ba}(\tilde{q}, \tilde{q}_{\max}; x, \tilde{q}_0) = \int_{\tilde{q}^2}^{\tilde{q}_{\max}^2} \frac{d\tilde{q}^2}{\tilde{q}^2} \int_{z_0}^{z_1} dz \frac{\alpha_S(z, \tilde{q}^2)}{2\pi} \frac{x' f_b(x', \tilde{q}^2)}{x f_a(x, \tilde{q}^2)} P_{ba}(z, \tilde{q}^2). \quad (2.2)$$

We assume a resolution scale \tilde{q}_0 below which the evolution terminates and further splittings would remain unresolvable. The limits of the z -integration, z_0 and z_1 depend implicitly on \tilde{q} and \tilde{q}_0 , hence the \tilde{q}_0 dependence¹ of \mathcal{I}_{ba} and S_a . x is the light cone momentum fraction of the parent parton with respect to the originating hadron. This value is initially selected by the hard subprocess. $x' = x/z$ is the light cone momentum fraction of the new parent after the first space like branching and so forth. $P_{ba}(z, \tilde{q}^2)$ is the unregularized collinear splitting function, which, in the case of the evolution of massive partons, may also depend on the branching scale \tilde{q}^2 . Note, that the splitting function is regularized as we use explicit cutoffs in the phase space for soft gluon emission. $f_a(x, \tilde{q}^2)$ is the parton distribution function (pdf) of a parton of type a inside a proton².

The integral in Eq. (2.2) is written in a fairly symbolic way and holds for different models. We shall rewrite it for the specific case of the kinematic variables that

¹Some authors prefer to stress this circumstance by writing S_{ba} as a ratio of two exponentials with explicit \tilde{q}_0 dependence in the \tilde{q} -integration. The two notations are, of course, equivalent.

²The conclusions will remain unchanged when considering antiprotons. The case of pions or resolved photons in the initial state is beyond the scope of this study.

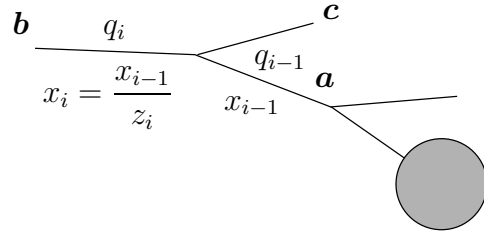


Figure 1: Kinematics for space-like branching $b \rightarrow ac$.

are used in **Herwig++** [14]. There, the evolution variables z, \tilde{q} are interpreted in a Sudakov basis. Consider the branching in Fig. 1. Each momentum is written as

$$q_i = \alpha_i p + \beta_i n + q_{\perp i} \quad (2.3)$$

where p and n are suitable forward and backward light like vectors, typically chosen along the axis of the original hadrons. Then we define our space-like branching kinematics via

$$\alpha_i = \frac{\alpha_{i-1}}{z}, \quad \mathbf{q}_{\perp i} = \frac{\mathbf{q}_{\perp i-1} - \mathbf{p}_{\perp i}}{z_i}. \quad (2.4)$$

Here, the relative transverse momentum $\mathbf{p}_{\perp i}$ is given in terms of the evolution variables \tilde{q} and z as

$$\mathbf{p}_{\perp i}^2 = (1 - z_i)^2 \tilde{q}_i^2 - z_i Q_g^2. \quad (2.5)$$

Q_g is the cutoff parameter of the parton shower. Choosing the argument of $\alpha_S(Q)$ as $Q = (1 - z_i)\tilde{q}_i$ we may now rewrite the integral (2.2) as

$$\mathcal{I}_{ba}(\tilde{q}, \tilde{q}_{\max}; x, Q_g) = \int_{\tilde{q}^2}^{\tilde{q}_{\max}^2} \frac{d\tilde{q}^2}{\tilde{q}^2} \int_0^1 dz \frac{\alpha_S[(1 - z)\tilde{q}]}{2\pi} \frac{x' f_b(x', \tilde{q}^2)}{x f_a(x, \tilde{q}^2)} P_{ba}(z, \tilde{q}^2) \Theta(\text{P.S.}). \quad (2.6)$$

The implicit introduction of the parton shower cutoff Q_g in (2.5) is reflected in the step function $\Theta(\text{P.S.})$. Hence we simply extend the integration region in z from 0 to 1 and apply this cut on the available parton shower phase space (see also Fig. 2). However, the resolution scale \tilde{q}_0 of the parton shower has disappeared and was implicitly replaced by Q_g . Now every given initial condition \tilde{q}_{\max}, x may result in different values of the resolution scale in terms of a smallest available scale. The shape of the available phase space

is, of course, still determined by Q_g in some intuitive way such that small cutoffs lead to a larger available phase space and a lower resolution scale. We set $Q_g \approx 1 \text{ GeV}$ if not stated otherwise³.

In practice, the available phase space is determined by some more factors. As we require a real transverse momentum we find the limits of the z integration for a

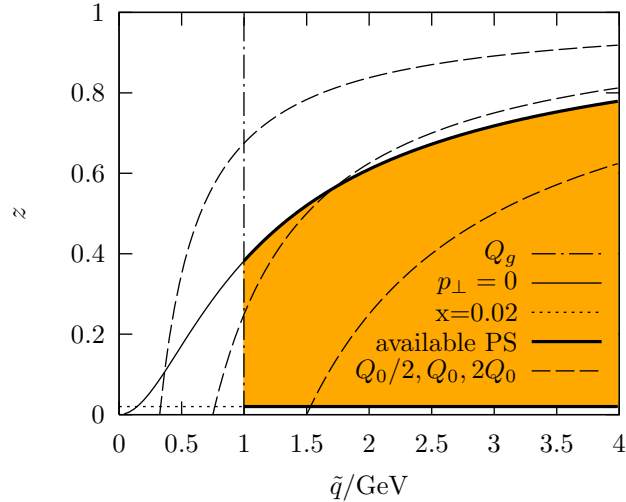


Figure 2: Available phase space for space-like branching.

³More precisely we choose the **Herwig++** parameter $\delta = 2.3 \text{ GeV}$ (cf. [6]). This leads to Q_g close to but slightly smaller than 1 GeV .

given \tilde{q} . As x' should never exceed 1, x itself is the lower limit of z . Therefore,

$$x < z < 1 + \frac{Q_g}{2\tilde{q}} - \sqrt{\left(1 + \frac{Q_g}{2\tilde{q}}\right)^2 - 1}. \quad (2.7)$$

Depending on the choice of how to evaluate $\alpha_S(Q)$ when Q becomes very small we have an additional constraint on the phase space. Let Q_0 be the scale where non-perturbative effects become important. Typically Q_0 is somewhat larger than but of the order of Λ_{QCD} . In order to model non-perturbative effects, we may simply freeze the value of α_S , $\alpha_S(Q < Q_0) = \alpha_S(Q_0)$. We set $Q_0 = 0.75 \text{ GeV}$ and freeze α_S by default. This gives us a behaviour of α_S very similar to the one in the MRST2001 parametrization [4] as we find it in [19]. If we put $\alpha_S(Q < Q_0) = 0$ we have an additional limitation of phase space. In Fig. 2 we show as an illustrative example the available phase space for $q \rightarrow qg$ spacelike branching with $\tilde{q}_{\text{max}} = 4 \text{ GeV}$ and $x = 0.02$ with its limiting regions. Lines of constant α_S for $Q_0/2, Q_0, 2Q_0$ are also shown.

We apply an extra cut at $\tilde{q} < Q_g$ in the rare cases where there is still phase space available. As the pdf's become unstable for Q values close to the non-perturbative domain we choose to freeze the pdf's at $Q_{\text{freeze}} = 2.5 \text{ GeV}$. The choice of this parameter is based on experience with HERWIG⁴.

In the following we consider the Sudakov form factor for specific branching types $b \rightarrow ac$ only. Formally we rewrite (2.1) as

$$S_a(\tilde{q}, \tilde{q}_{\text{max}}; x, Q_g) = \prod_b S_{ba}(\tilde{q}, \tilde{q}_{\text{max}}; x, Q_g) \quad (2.8)$$

where $S_{ba} = \exp -\mathcal{I}_{ba}$. Then we only consider specific S_{ba} . For the parton shower evolution the Sudakov form factor is interpreted as the probability that the parton a remains unresolved upon evolution from \tilde{q}_{max} down to \tilde{q} when the minimal resolution is \tilde{q}_0 . With the probability $1 - S_{ba}$ that there is any branching between \tilde{q}_{max} and \tilde{q} we find the branching probability density

$$\mathcal{P}_{ba}(\tilde{q}, \tilde{q}_{\text{max}}; x, Q_g) = \mathcal{I}'_{ba}(\tilde{q}; x, Q_g) S_{ba}(\tilde{q}, \tilde{q}_{\text{max}}; x, Q_g), \quad (2.9)$$

where $\mathcal{I}'_{ba}(\tilde{q}; x, Q_g)$ is the integrand of (2.6) with respect to the \tilde{q} integration. The scales of the next branching \tilde{q} are distributed according to $\mathcal{P}_{ba}(\tilde{q}, \tilde{q}_{\text{max}}; x, Q_g)$. This is the quantity we would like to consider in order to estimate uncertainties of different types as it is directly implemented in parton shower Monte Carlo programs. We should note that $\mathcal{P}_{ba}(\tilde{q}, \tilde{q}_{\text{max}}; x, Q_g)$ is normalized to

$$\int_{\tilde{q}_{\text{max}}}^{\tilde{q}_0} \mathcal{P}_{ba}(\tilde{q}, \tilde{q}_{\text{max}}; x, Q_g) d\tilde{q} = 1 - S_{ba}(\tilde{q}_0, \tilde{q}_{\text{max}}; x, Q_g). \quad (2.10)$$

This is typically different from 1 as we have a chance $S_{ba}(\tilde{q}_0, \tilde{q}_{\text{max}}; x, Q_g)$ to find no branching at all. Their sum is obviously one.

⁴In HERWIG the pdf's are regularized by the parameter QSPAC with the default value 2.5 GeV.

3. Numerical study

For numerical purposes we map the integration variables \tilde{q} and z onto new variables t, y as

$$t = \ln \tilde{q}^2, \quad y = \ln \frac{z}{1-z}, \quad (3.1)$$

in order to absorb the leading poles into the integration variables,

$$dt = \frac{d\tilde{q}^2}{\tilde{q}^2}, \quad dy = \frac{dz}{z(1-z)}. \quad (3.2)$$

We carry out the integrations in $\mathcal{I}'_{ba}(\tilde{q}; x, Q_g)$ and $\mathcal{I}_{ba}(\tilde{q}, \tilde{q}_{\max}; x, Q_g)$ numerically with adaptive Gaussian or Monte Carlo algorithms [15, 16, 17]. Different packages have been used for consistency checks. Particular care has been taken to obtain numerical results with a typical relative error of at least one order of magnitude below the resulting pdf errors as the former ones would mask the latter ones otherwise.

In the following we address the uncertainties of Sudakov form factors that arise from various sources. As we do not aim at a study of Sudakov form factors beyond leading logarithmic accuracy, the sources of uncertainties are:

1. the ratio of pdf's, which may even be pdf's of different flavour in the case of $q \rightarrow gq$ and $g \rightarrow q\bar{q}$ branching,
2. parametrization of the running of α_S may play an important rôle,
3. modelling of α_S in the non-perturbative region below our choice of Q_0 .

Recently, the uncertainties of parton distribution functions have been considered for various observables and the question has been raised how much of an influence they would have on Monte Carlo showering algorithms [18].

In order to assess the relevance of uncertainties arising from the parton distribution functions we basically follow the procedure described in [4] and [5]. We obtain the integral once for the central pdf fit and once for all the error members. The variations from each pair of error pdf's are added in quadrature and thus we obtain an error estimate $\delta\mathcal{I}_{ba}$ for the integral from which we can derive the uncertainty in the probability distribution 2.9. All calculations have been performed with the pdf error distributions from MRST and CTEQ [4, 5] as they are provided in [19].

The parametrization of the running of $\alpha_S(Q)$ may give important differences in the result. Particularly as different orders of the running result in large deviations at smaller values of Q . In Fig. 3 we show our default parametrization with and without freezing as well as the MRST parametrization of $\alpha_S(Q)$. By default we use the two-loop α_S that is implemented in **Herwig++**. We choose to freeze α_S at $Q_0 = 0.75$ GeV as discussed above. This parametrization is numerically very close to that of MRST. The parametrization of the α_S in the CTEQ distribution is very similar but does not

model α_S at small scales Q in some particular way. We therefore do not check this parametrization explicitly. For MRST we compared results from a computation with the given pdf set where by default we use our own parametrization of α_S with the same computation where the α_S is taken from the distribution of the pdf set itself.

As the results seemed to be fairly sensitive on the choice of α_S -parametrization we have also checked the effect of setting α_S to zero below Q_0 . This may have drastic consequences as one can see with the help of Fig. 2. There, we plotted lines of constant Q_0 once for the central value and once the values resulting from rescaling by factors of 2. We see that we may cut out regions in phase space that actually give very large contributions to the integral \mathcal{I}_{ba} . For estimates of this scale uncertainty we compute the Sudakov form factors and the branching probability densities with variation of the scale by a factor two.

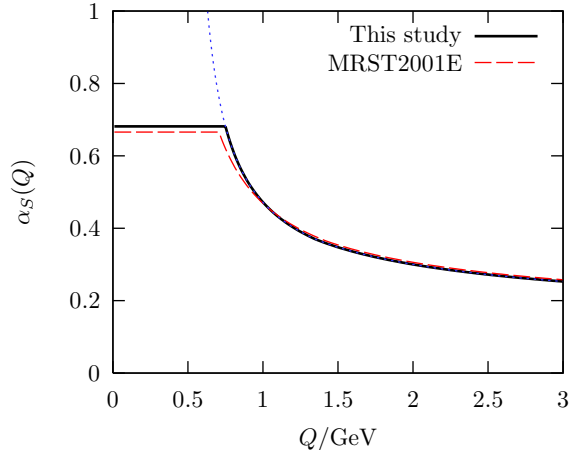


Figure 3: Different parametrizations of $\alpha_S(Q)$.

4. Results

We consider the Sudakov form factors and branching probability densities in the following. We choose different initial conditions \tilde{q}_{\max}, x for the evolution and focus on a particular type of branching at a time. The plots contain three panels and show S_{ba} on top, \mathcal{P}_{ba} in the middle and some error information on the bottom panel.

4.1 Different initial conditions

We first consider different initial conditions and branching types. In this case we always use MRST partons. We plot Sudakov form factor and branching probability density for a number of different initial conditions. The error box in the lowest panel always compares the error from the numerical integration with the total error that also contains the pdf error itself. This is to control that the numerical error is negligible compared to the pdf error. This is always the case as the numerical error is typically two orders of magnitude smaller than the pdf error.

In Fig. 4 we show the uncertainties in the case of $q \rightarrow qg$ spacelike branching. We pick d quarks in particular. Clearly, the estimated pdf error is by far smaller than the one from varying the α_S scale by a factor of two. Generally, the pdf uncertainty is largest at small initial scales $\tilde{q}_{\max} = 10$ GeV and somewhat larger at small x . This goes along with the fact that the quark densities are known better at large x than at

small x . We do not show any plots at intermediate values of x and \tilde{q} as they do not exhibit any new features. The plots shown in Fig. 4 are those with a large visible effect.

For $g \rightarrow gg$ branchings we get a slightly different picture in Fig. 5. The pdf uncertainties are much larger in this case as the gluon density is not as much constrained as the valence quark density. This is particularly true at large x . Going to small $x = 10^{-4}$ at $\tilde{q}_{\max} = 10$ GeV the pdf uncertainty is very large (the largest we encounter in this study) and sometimes even larger than the uncertainty from α_S scale variation. This is still the case if one goes to a larger initial $\tilde{q}_{\max} = 30$ GeV but the effect is still largest at small target values of \tilde{q} . For even larger \tilde{q}_{\max} (not shown) we observe the same trend.

We also consider the more unlikely branchings $g \rightarrow gq$ and $g \rightarrow q\bar{q}$ in Fig. 6. The Sudakov form factor for these branchings is typically close to one. The pdf uncertainties can be sizable as well, particularly when we involve a gluon at small values of x where we also had the largest uncertainty in the case of $g \rightarrow gg$ splitting. Still, we have selected situations with particularly large pdf uncertainties. Generally, we have the larger error from α_S scale variation.

In Fig. 7 we replace the initial valence quark $a = d$ with a sea quark $a = \bar{d}$. Now we can directly observe and compare the sea-like behaviour of the \bar{d} as opposed to the valence d -quark. Especially at larger $x = 0.1$ the evolution clearly prefers valence quarks (note, that the branching probability density is normalized to the total probability of such a branching to occur). We can directly compare to the picture at small $x = 10^{-3}$ where the two distributions begin to coincide as the valence structure loses its dominance. The opposite happens of course for evolution *away* from the d/\bar{d} into a gluon. The evolution of the d is clearly suppressed. As far as the errors due to pdf's are concerned we observe that the uncertainty of the sea quark density at large x becomes visible as it does for the gluon. This is highly emphasised at the low end of the evolution.

4.2 MRST vs CTEQ

As an obvious cross check we repeated all computations also with the CTEQ6m error set. In Fig. 8 we show some of the previous plots again, without α_S uncertainties, comparing the error bands of the two parton distribution packages. We find that the distributions are compatible but the error estimates from CTEQ are smaller, particularly for gluons at small x . Again, we have picked cases that show clear differences. Generally, both packages tend to give similar (and compatible) results.

4.3 Parametrization of α_S

As already pointed out in the discussion of the available phase space, the effect of different parametrizations of $\alpha_S(Q)$, especially at low Q can have important effects. In Fig. 9 we show the effect of using the α_S parametrization that is provided via

the distribution of MRST itself with our parametrization. We have chosen a very similar regularisation for non-perturbative values of α_S as MRST have. Therefore the results are very similar, nevertheless they are sensitive to the small differences in the parametrization of α_S . However, the effect of using a parametrization that sets α_S to zero below e.g. $Q_0 = 0.75 \text{ GeV}$ leads to a very different result as effectively a part of phase space is modified in which \mathcal{I}_{ba} picks up very large contributions. This is of particular importance when we use $Q/2$ as this cuts out a lot of phase space. In the other two cases the results closely follow those of our default parametrization until they hit the phase space boundary.

4.4 Larger cutoff

As a final subject we consider the spacelike evolution of light quarks or gluons at large $x = 0.2$ and fairly high initial scale $\tilde{q}_{\text{max}} = 250 \text{ GeV}$. This situation can give us some information about the initial state radiation in top production at hadron colliders. $t\bar{t}$ pairs are predominantly produced from light quark scattering at large x . The relevant initial scale \tilde{q}_{max} is given by a typical invariant mass in the t -channel as the colour connection is between one initial light quark and one t -quark [14]. This gives us a typical initial scale $\tilde{q}_{\text{max}} = 250 \text{ GeV}$.

In Fig. 10 we have plotted the relevant Sudakov form factors and branching probability densities for such a situation. We have increased the cutoff scale to higher values $Q_g = 2.5 \text{ GeV}$ and/or 10 GeV . This allows us to directly estimate the effect of the radiation of an extra gluon at a fairly large (visible) scale. We find that the pdf uncertainties remain fairly low in the Sudakov form factors themselves. The size of the branching probability distribution is affected to some extent but the shape is hardly modified. Again, the uncertainty from the variation of α_S is much larger.

5. Conclusion

We have studied the effect of various sources of uncertainties on the parton shower evolution. We therefore particularly considered the branching probability density as this is the quantity that drives the evolution. We generally find that the effect of pdf uncertainties is small compared to uncertainties in the QCD description of the evolution itself that we estimate via scale variation in the strong coupling. There are, however, particular regions in phase space where the pdf uncertainties are very large. This is the case for the evolution from very small values of x and also at large x when sea quarks or gluons are involved. Considering the initial conditions in \tilde{q} we find that the pdf uncertainties are generally small when the initial conditions are in the large \tilde{q} regime. In the course of the parton shower evolution, however, all showers have to evolve through the small \tilde{q} in some way. Besides, we emphasise that the evolution strongly depends on the modelling of α_S in the transition region between

perturbative and non-perturbative QCD. This uncertainty is, however, usually taken as a sensitivity that is exploited in tuning Monte Carlo showers to experimental data.

In summary, we find that one should be aware of pdf uncertainties in the evolution when one is confined to a phase space of fairly large x and relatively small initial \tilde{q} .

Acknowledgments

I would like to thank J. Huston for fruitful conversations and for raising this topic at the HERA/LHC workshop. I also thank Peter Richardson, Mike Seymour and Bryan Webber for valuable comments.

References

- [1] G. Marchesini and B. R. Webber, Nucl. Phys. B **310**, 461 (1988).
- [2] T. Sjostrand, Phys. Lett. B **157**, 321 (1985).
- [3] R. K. Ellis, W. J. Stirling and B. R. Webber, “QCD and Collider Physics,” Cambridge Monogr. Part. Phys. Nucl. Phys. Cosmol. **8** (1996) 1.
- [4] A. D. Martin, R. G. Roberts, W. J. Stirling and R. S. Thorne, Eur. Phys. J. C **28** (2003) 455 [arXiv:hep-ph/0211080].
- [5] J. Pumplin, D. R. Stump, J. Huston, H. L. Lai, P. Nadolsky and W. K. Tung, JHEP **0207** (2002) 012 [arXiv:hep-ph/0201195].
- [6] S. Gieseke, A. Ribon, M. H. Seymour, P. Stephens and B. Webber, JHEP **0402**, 005 (2004) [arXiv:hep-ph/0311208].
- [7] G. Corcella *et al.*, “HERWIG 6.5 release note,” arXiv:hep-ph/0210213;
G. Corcella *et al.*, “HERWIG 6: An event generator for hadron emission reactions with interfering gluons (including supersymmetric processes),” JHEP **0101** (2001) 010 [arXiv:hep-ph/0011363].
- [8] T. Sjostrand, L. Lonnblad, S. Mrenna and P. Skands, “PYTHIA 6.3 physics and manual,” arXiv:hep-ph/0308153; T. Sjostrand, P. Eden, C. Friberg, L. Lonnblad, G. Miu, S. Mrenna and E. Norrbin, “High-energy-physics event generation with PYTHIA 6.1,” Comput. Phys. Commun. **135** (2001) 238 [arXiv:hep-ph/0010017].
- [9] T. Gleisberg, S. Hoche, F. Krauss, A. Schalicke, S. Schumann and J. C. Winter, JHEP **0402** (2004) 056 [arXiv:hep-ph/0311263].
<http://www.physik.tu-dresden.de/~krauss/hep/>.
- [10] S. Catani, F. Krauss, R. Kuhn and B. R. Webber, JHEP **0111** (2001) 063 [arXiv:hep-ph/0109231];

- [11] F. Krauss, JHEP **0208** (2002) 015 [arXiv:hep-ph/0205283].
- [12] S. Mrenna and P. Richardson, JHEP **0405** (2004) 040 [arXiv:hep-ph/0312274].
- [13] F. Krauss, A. Schalicke, S. Schumann and G. Soff, Phys. Rev. D **70** (2004) 114009 [arXiv:hep-ph/0409106].
- [14] S. Gieseke, P. Stephens and B. Webber, JHEP **0312**, 045 (2003) [arXiv:hep-ph/0310083].
- [15] W.H. Press, B.P. Flannery, S.A. Teukolsky, W.T. Vetterling, Numerical Recipes in C, Cambridge University Press, 1992.
- [16] <http://www.gnu.org/software/gsl/>
- [17] T. Hahn, arXiv:hep-ph/0404043.
- [18] J. Huston, private communication.
- [19] <http://durpdg.dur.ac.uk/lhapdf/>

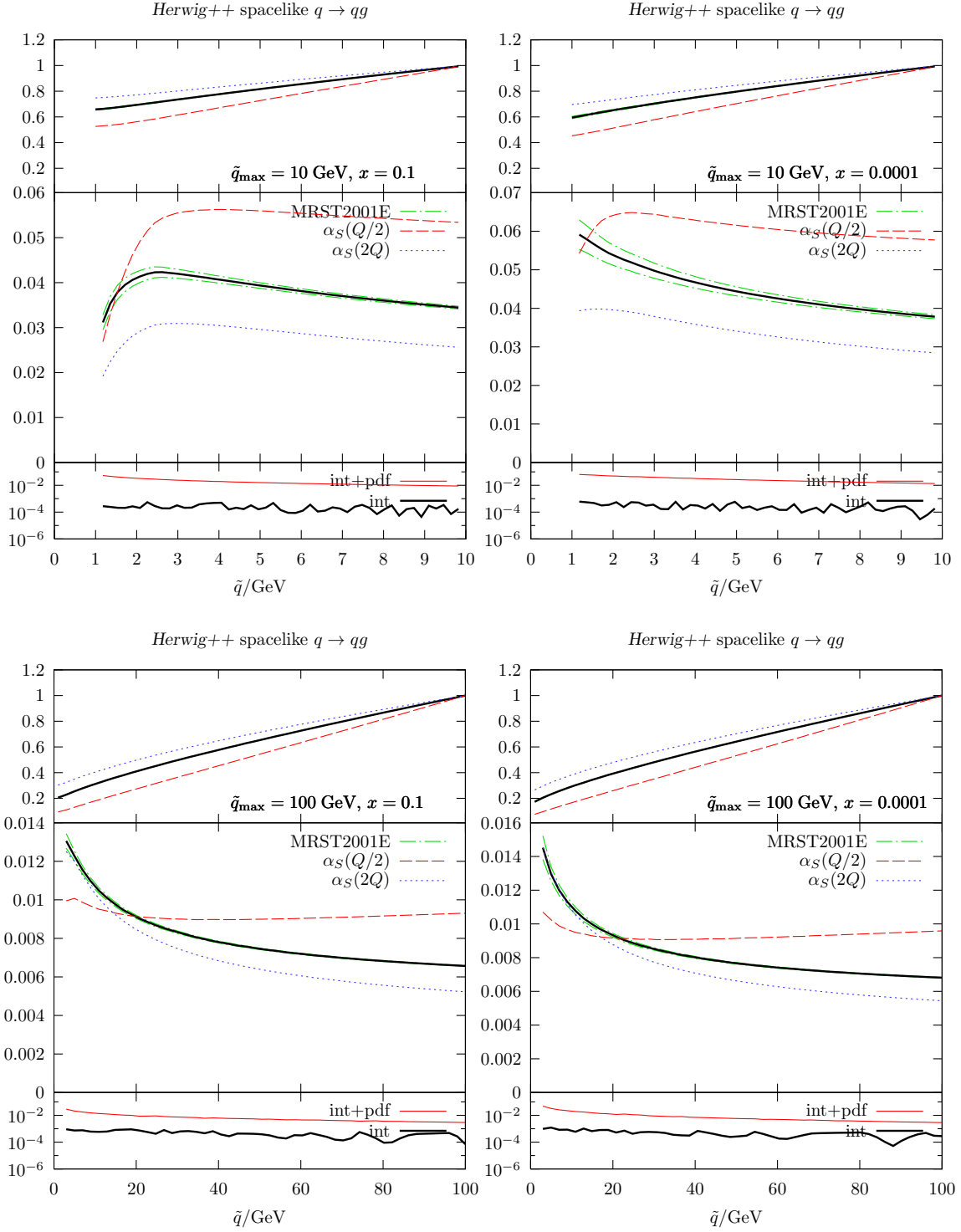


Figure 4: pdf and α_S uncertainties in spacelike $q \rightarrow qq$ branchings for different initial conditions \tilde{q}_{\max} and x . Each plot shows $S_{ba}(\tilde{q})$ (top), $\mathcal{P}_{ba}(\tilde{q})$ (middle) and the relative error $\delta\mathcal{P}_{ba}/\mathcal{P}_{ba}$ from numerical integration and pdf uncertainties (bottom panel). The central value is shown as solid line, central \pm pdf error is dot-dashed and α_S uncertainties from rescaling the argument by a factor $1/2$ and 2 are shown as dashed/dotted line, respectively.

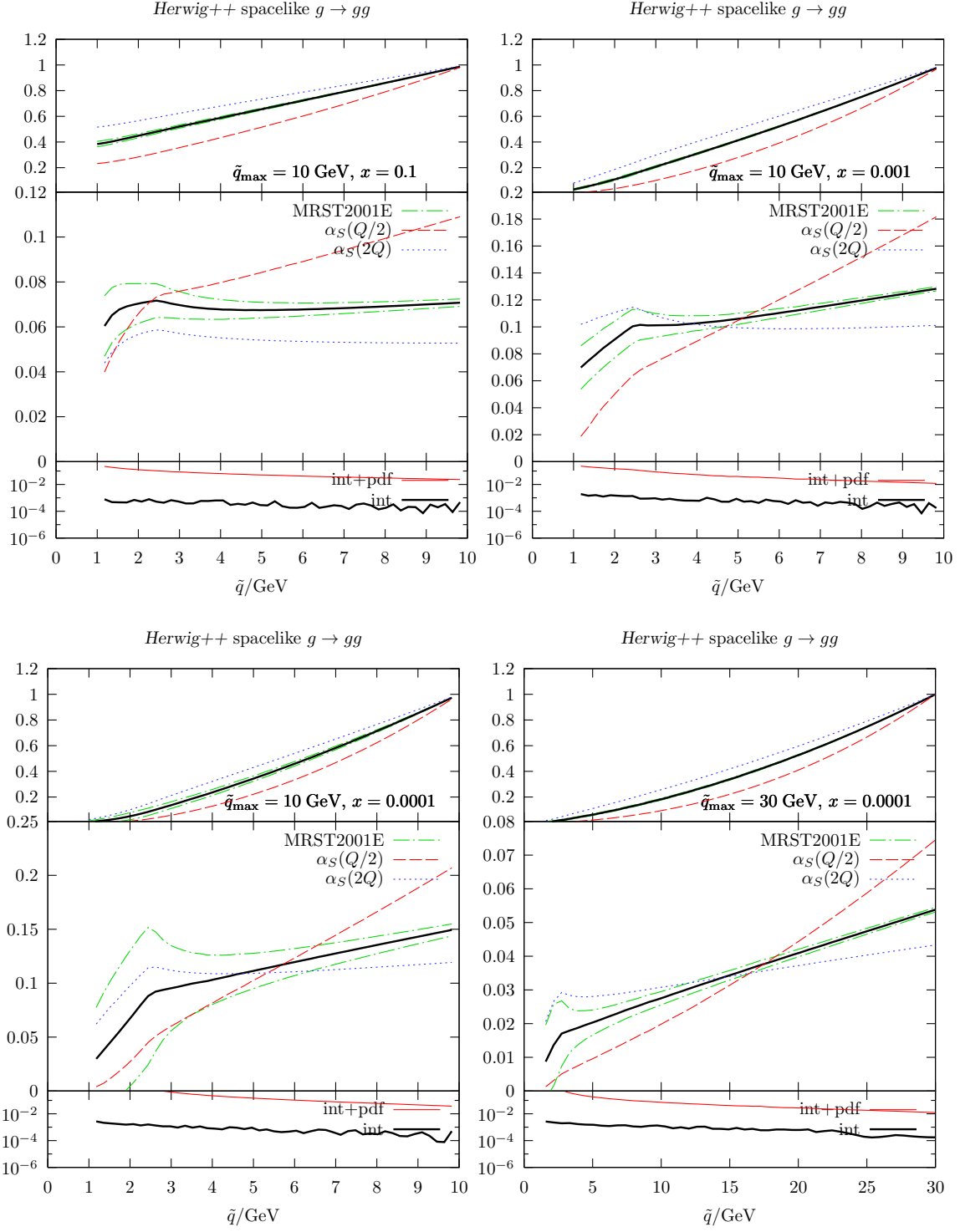


Figure 5: pdf and α_S uncertainties in spacelike $g \rightarrow gg$ branchings at different x and \tilde{q}_{\max} values. See caption of Fig. 4 for labelling.

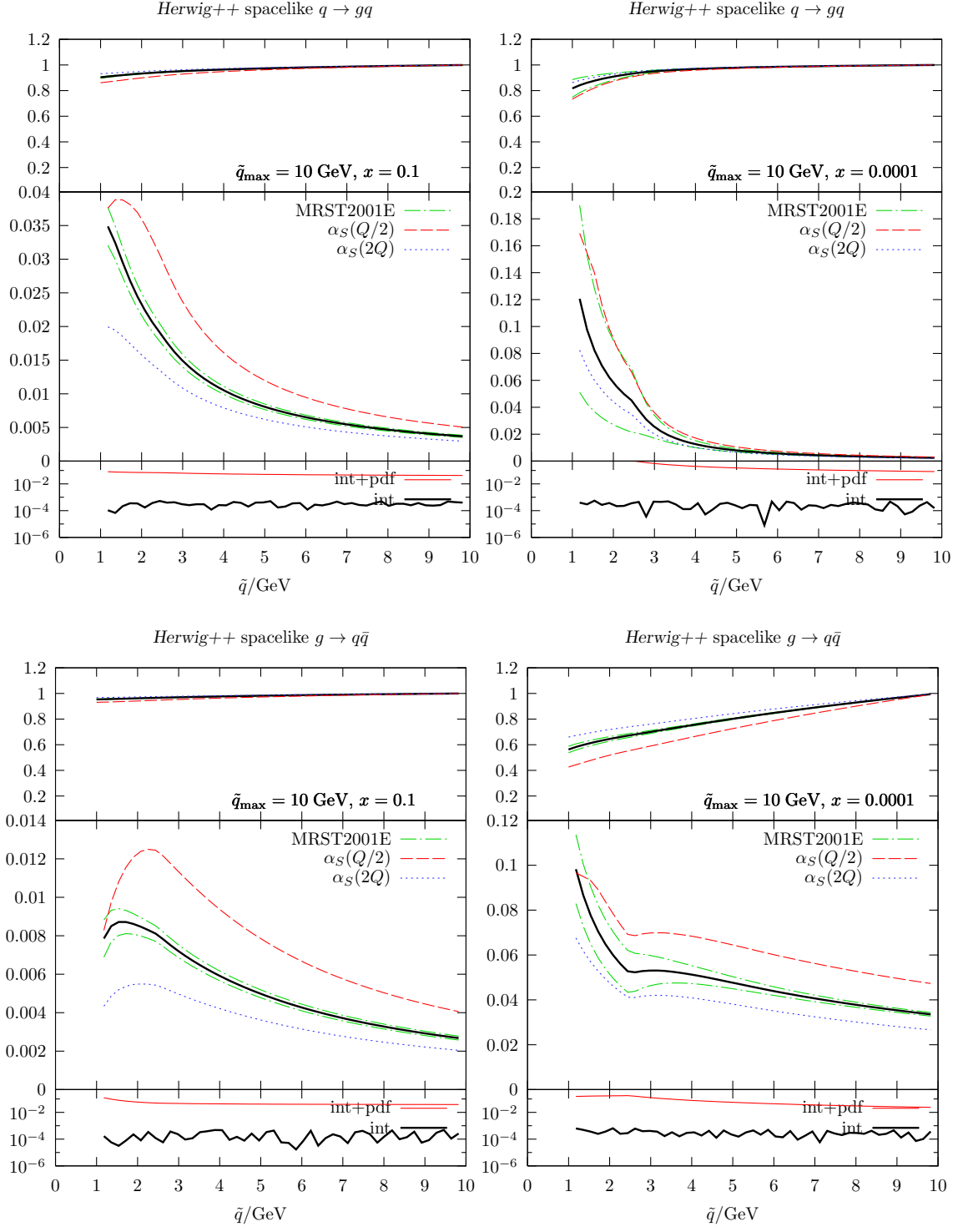


Figure 6: pdf and α_S uncertainties of the branchings $q \rightarrow gq$ and $g \rightarrow q\bar{q}$ at different x -values. See caption of Fig. 4 for labelling.

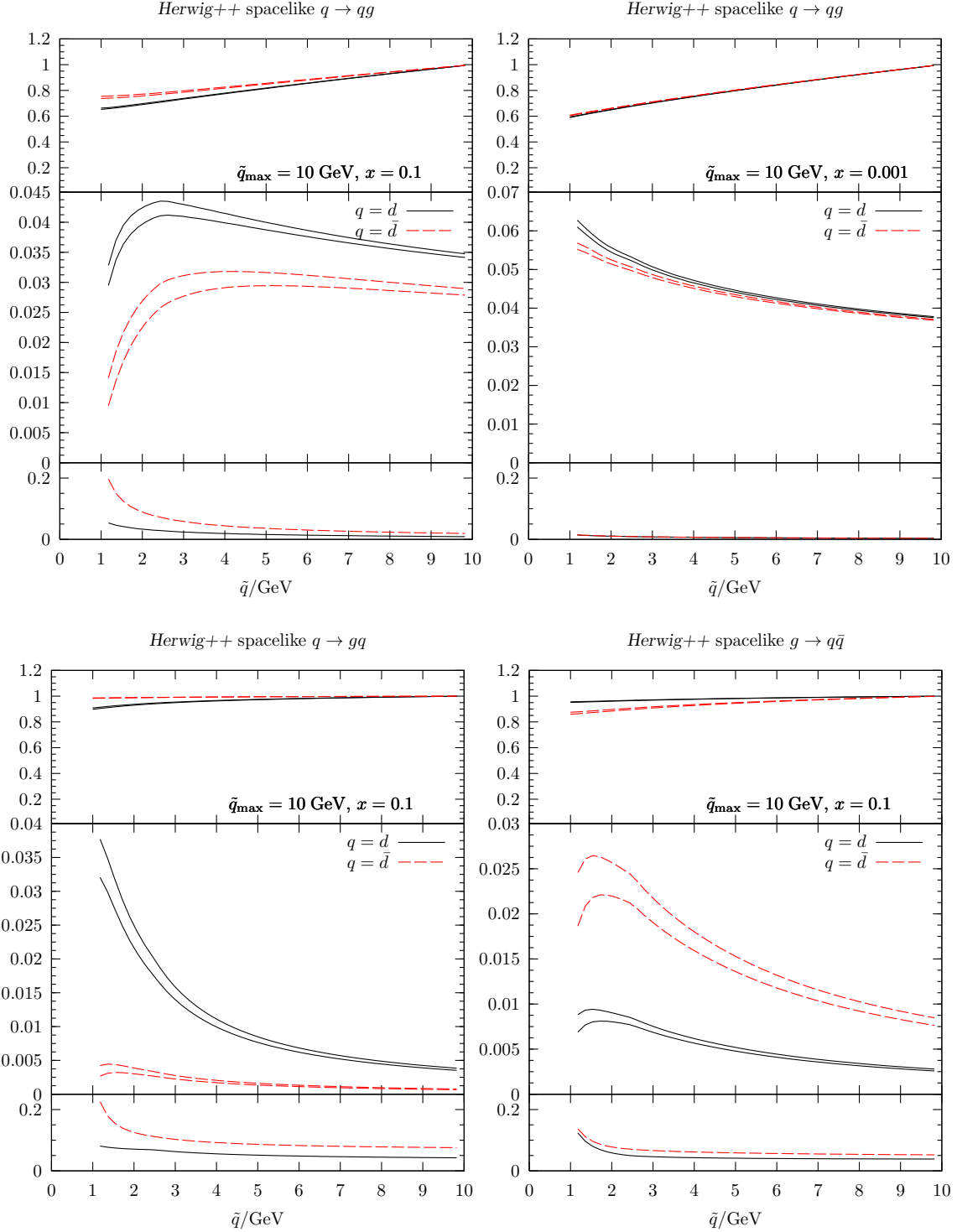


Figure 7: Comparison of uncertainties in the evolution of valance (d) quarks and sea (\bar{d}) quarks. The lowest panels show the total relative error of the branching probability densities. The solid lines are partly identical to the pdf error bands in Figs. 4 and 6. See caption of Fig. 4 for labelling.

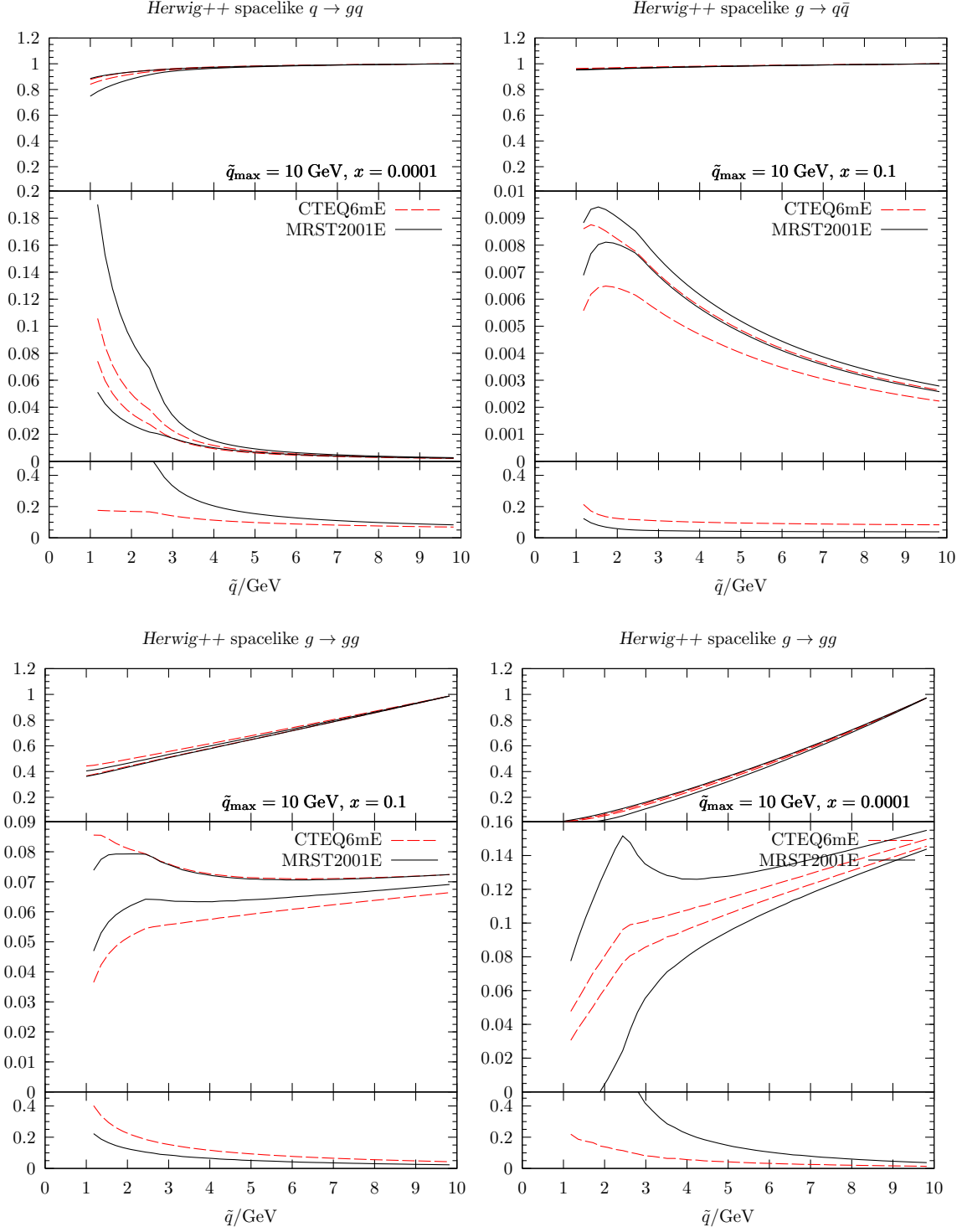


Figure 8: Comparison of pdf uncertainties from MRST2001E (solid) and CTEQ6mE (dashed) parametrizations where differences are most significant. Upper and middle panel are similar to Fig. 4. The bottom panel shows the relative pdf error of the branching probability density. See caption of Fig. 4 for labelling.

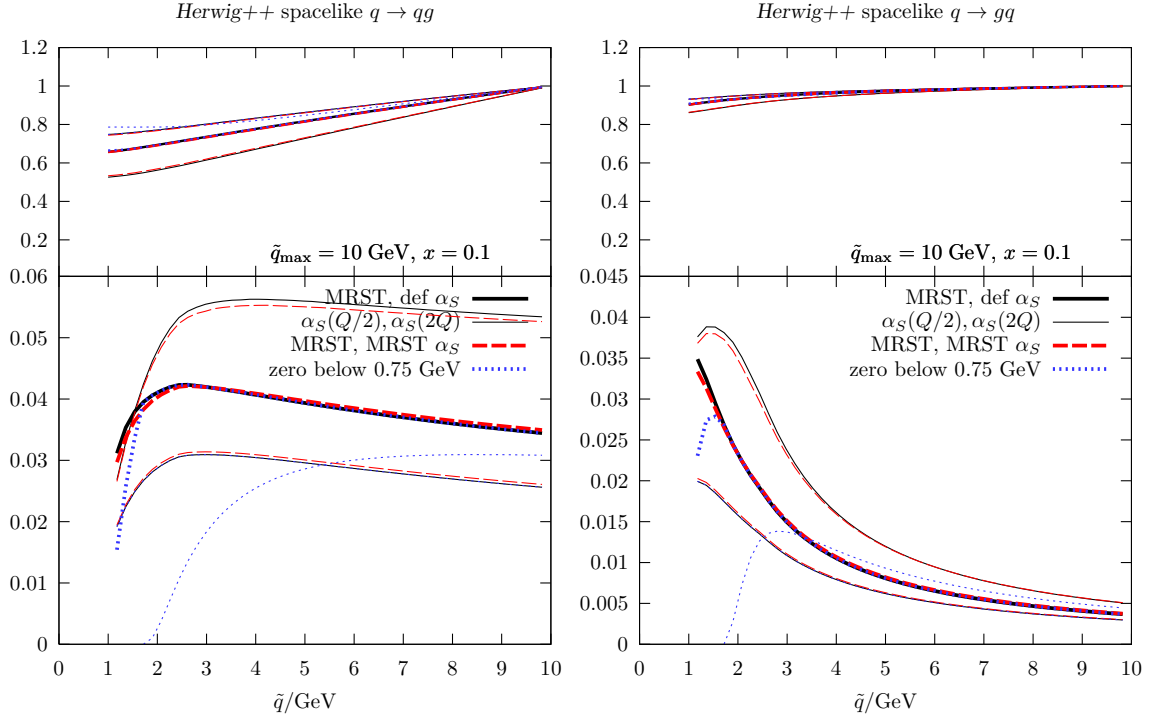


Figure 9: Effect of different α_S parametrizations in spacelike $q \rightarrow qq$ and $q \rightarrow gq$ branchings. The solid line in both plots denotes the previous results, obtained with MRST partons and our default parametrization of α_S , including the effect of varying the scale by a factor of 2. The dashed and dotted lines are results obtained with different parametrizations of α_S .

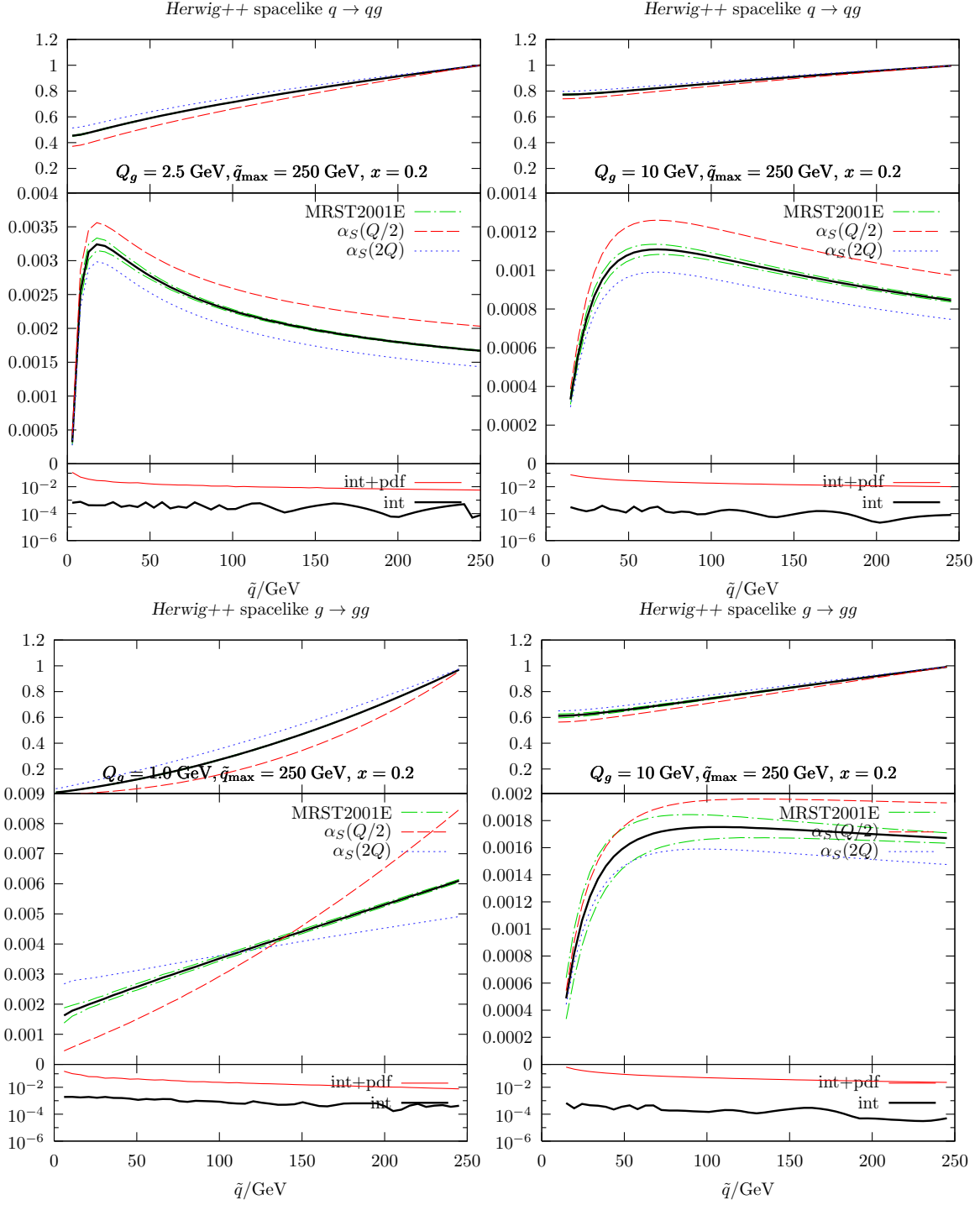


Figure 10: Increasing the cutoff Q_g in the $q \rightarrow qg$ and $g \rightarrow gg$ Sudakov form factors for at large \tilde{q}_{\max} and x . See caption of Fig. 4 for labelling.